Biochemical and Biophysical Research Communications 431 (2013) 554–559

Contents lists available at SciVerse ScienceDirect

Biochemical and Biophysical Research Communications

journal homepage: www.elsevier.com/locate/ybbrc

pH-dependent structural change of the extracellular sensor domain of the DraK histidine kinase from *Streptomyces coelicolor*

Kwon Joo Yeo [a], Eun Hye Kim [b], Eunha Hwang [a], Young-Hyun Han [a], Yumi Eo [a], Hyun Jung Kim [a], Ohsuk Kwon [b], Young-Soo Hong [c], Chaejoon Cheong [a,*], Hae-Kap Cheong [a,*]

[a] Division of Magnetic Resonance, Korea Basic Science Institute (KBSI), 16 Yeongudanji-Ro, Ochang, Chungbuk 363-883, Republic of Korea
[b] Systems and Synthetic Biology Research Center, Korea Research Institute of Bioscience and Biotechnology (KRIBB), 125 Gwahak-Ro, Yuseong-Gu, Daejeon 305-333, Republic of Korea
[c] Chemical Biology Research Center, KRIBB, 30 Yeongudanji-Ro, Ochang, Chungbuk 363-883, Republic of Korea

ARTICLE INFO

Article history:
Received 22 December 2012
Available online 12 January 2013

Keywords:
DraK
SCO3062
pH-sensitive histidine kinase
pH-dependent conformational change
Sensory domain
Streptomyces coelicolor
Two-component system

ABSTRACT

Recently, the DraR/DraK (Sco3063/Sco3062) two-component system (TCS) of *Streptomyces coelicolor* has been reported to be involved in the differential regulation of antibiotic biosynthesis. However, it has not been shown that under which conditions and how the DraR/DraK TCS is activated to initiate the signal transduction process. Therefore, to understand the sensing mechanism, structural study of the sensory domain of DraK is highly required. Here, we report the biochemical and biophysical properties of the extracellular sensory domain (ESD) of DraK. We observed a reversible pH-dependent conformational change of the ESD in a pH range of 2.5–10. Size-exclusion chromatography and AUC (analytical ultracentrifugation) data indicated that the ESD is predominantly monomeric in solution and exists in equilibrium between monomer and dimer states in acidic condition. Using NMR (nuclear magnetic resonance) and CD (circular dichroism) spectroscopy, our findings suggest that the structure of the ESD at low pH is more structured than that at high pH. In particular, the glutamate at position 83 is an important residue for the pH-dependent conformational change. These results suggest that this pH-dependent conformational change of ESD may be involved in signal transduction process of DraR/DraK TCS.

1. Introduction

Two-component systems (TCSs) ubiquitously exist in various organisms from prokaryotes and archaea to some eukaryotes, such as fungi and plants, but not in animal cells. This system may be a potential drug target for antibiotics [1]. TCSs serve in bacterial signal transduction for cellular adaptation to external stimuli and stresses, such as osmolarity, ionic strength, pH, redox states, quorum signals, harmful compounds, temperature, wavelength of light, and nutrient concentrations [2–4]. Typically, TCSs consist of a membrane-associated histidine kinase (HK), which functions as a homodimer, and its cognate response regulator (RR). HKs are composed of an N-terminal sensory (or input) domain, which senses external stimuli, and a conserved kinase domain, which contains an N-terminal dimerization and histidine phosphotransfer (His KA) domain and a catalytic and ATP (adenosine triphosphate) binding (CA) domain. In contrast, RRs, which are composed of an N-terminal receiver domain and a C-terminal output domain, control the cellular response through protein–protein interactions or protein–DNA interactions modulating its target gene expression.

Focusing on the sensory domain of HKs, it is typically composed of 100–200 amino acid residues but there is low sequence homology for this domain among HKs. This lack of overall sequence conservation is thought to enable sensing of variable external signals. This wide range of input signals impedes the functional and structural studies of these sensory domains. Thus, sensory domains may serve as potential drug targets because their input specificity may be exploited to develop specific inhibitors of specific TCS signaling pathways [1]. Although the functions of some HKs are known, the functions of many HKs remain unknown, and only a few structures of sensory domains have been elucidated [5,6].

Streptomyces coelicolor A3(2) is the best known representative of the genus *Streptomyces* and a Gram-positive soil bacterium that exhibits a complex life cycle and metabolic processing that is responsible for producing secondary metabolites [7,8]. The information of *S. coelicolor* has provided valuable clues for better understanding and rational manipulation of other industrially or medically important *Streptomycetes*. Recently, the complete genome sequence of this organism has been published [7]. From the genome sequence, TCSs containing 84 HKs and 80 RRs were revealed [9]. Of 84 HK genes, 67 are shown to be adjacent to RR genes

* Corresponding authors. Fax: +82 43 240 5059.
E-mail addresses: cheong@kbsi.re.kr (C. Cheong), haekap@kbsi.re.kr (H.-K. Cheong).

0006-291X/$ - see front matter © 2013 Elsevier Inc. All rights reserved.
http://dx.doi.org/10.1016/j.bbrc.2013.01.018

on the chromosome, whereas the remaining 17 HK genes are unpaired. However, the functions of most of these TCSs remain unknown, and only a few of them have been functionally characterized [10–19].

More recently, it was reported that the DraR/DraK TCS of *S. coelicolor* regulates the differential production of antibiotics [19]. In the report, in minimal medium with a high concentration of nitrogen sources such as glutamine, glutamate, threonine, and $(NH_4)_2SO_4$, DraR/K was shown to activate the biosynthesis of actinorhodin (ACT) and repress production of a yellow-pigmented type I polyketide (yCPK) and undecylprodigiosin (RED). Nevertheless, the signal molecule of DraK remains unknown, and the structural properties of the sensor domain have not been characterized. Therefore, the structural study of the DraR/DraK of TCS is of interest not only to determine the signal molecule but also to understand how to regulate the biosynthesis of various antibiotics in *S. coelicolor*.

Here, we report the structural properties of the ESD of DraK and a phosphorylation assay for the DraR/DraK TCS in vitro. We hope that our results will aid in the elucidation of the understanding of the signaling mechanism of the DraK HK.

2. Materials and methods

2.1. Cloning, expression, and purification

The DNA fragments encoding the ESD (28E-124R), the cytoplasmic domain (146R-424R)of DraK, and the full length DraR were amplified from the genomic DNA of *S. coelicolor* A3(2) (ATCC BAA471D) by polymerase chain reaction (PCR). All PCR products were cloned into the pGEX-4T-1 expression vector, which resulted in the expression of the proteins fused to a GST (glutathione *S*-transferase-binding protein) fusion tag at their N-termini. The plasmids were transformed into the *Escherichia. coli* BL21 strain, and transformants were grown overnight in 50 mL of Luria–Bertani (LB) broth at 37 °C. A 10 mL preculture was inoculated into 1 L of LB broth in a 2.5 L baffled flask, and the cells were grown at 37 °C with shaking at 120 rpm until an OD_{600} of 0.6–0.8. After decreasing the temperature to 18 °C, the proteins were induced with 0.2 mM isopropyl β-D-thiogalactopyranoside (IPTG). The cells were grown for 18–20 h at 18 °C following the addition of IPTG. All growth media were supplemented with 100 μg/mL ampicillin. The cells harvested by centrifugation at 3000 g for 30 min at 4 °C were resuspended in phosphate-buffered saline (PBS) containing 1 mM ethylenediaminetetraacetic acid (EDTA), 2 mM phenylmethylsulfonyl fluoride (PMSF), and one tablet of protease inhibitor cocktail (Roche) and then lysed using a sonicator. Insoluble inclusion bodies and cell debris were removed by centrifugation at 10,000 g for 30 min. The soluble fractions were loaded onto a 5 mL GST column (GE Healthcare), and impurities and unbound proteins were removed by washing with 5 column volumes (CV) of PBS buffer. The target proteins were eluted with elution buffer containing 50 mM Tris–HCl, pH 8.0, 100 mM NaCl, and 10 mM reduced glutathione. The eluted proteins were incubated at 4 °C overnight following the addition of thrombin to cleave the GST fusion tag. The GST fusion tag was then removed by size-exclusion chromatography using a prep-grade HiLoad 16/60 Superdex 75 column (GE Healthcare) connected to a 5 mL GST column in series that was equilibrated with a proper buffer. All purification steps were performed at 4 °C. To determine the molecular mass of the target protein by size-exclusion chromatography using a Superdex 75 column equilibrated with a buffer containing 100 mM NaCl, standard molecular weight markers (Ribonuclease A, 13,700 Da; chymotrypsinogen, 25,000 Da; ovalbumin, 43,000 Da; albumin, 67,000 Da) were used.

2.2. Analytical ultracentrifugation (AUC)

Sedimentation equilibrium measurements were performed using a Beckman XL-I analytical ultracentrifuge (Beckman Coulter, Fullerton, CA) at 30,000 rpm at 4 °C with a 0.2 mM concentration of the sESD of DraK in the presence of 50 mM NaCl for both pH 4.5 (20 mM sodium acetate) and pH 7.5 (20 mM Tris–HCl). The samples were centrifuged for specific time periods to achieve equilibrium. Data were collected by UV absorption at 280 nm and the molecular mass of the protein was determined by nonlinear least-squares curve fitting using the program Sedphat.

2.3. Circular dichroism (CD) spectroscopy

CD spectra were acquired using a J-710 spectropolarimeter (JASCO) with a cylindrical quartz cell with a path length of 1 mm. Data were acquired at a scan rate of 0.2 nm/s, and data from five scans were averaged. The sESD of DraK was used at a concentration of 30 μM for measurement. For CD spectra at different pH values, samples were titrated using microliter aliquots of 0.05–0.1 M of either HCl or NaOH following dialysis in distilled and deionized water at approximately pH 3.0 in the presence of 50 mM NaCl. The transition point of the pH-dependent conformational change was determined by sigmoidal curve fitting using the program Origin 8.0 (OriginLab).

2.4. NMR sample preparation

For ^{15}N-labeled NMR samples, *E. coli* containing the plasmid for expression of the sESD of DraK were grown in M9 minimal medium supplemented with $^{15}NH_4Cl$ as the sole nitrogen source (99% ^{15}N; Cambridge Isotope Laboratories, Inc.) at 37 °C until the OD_{600} was approximately 0.8. After decreasing the temperature to 18 °C, the protein was induced by the addition of 0.5 mM IPTG. The subsequent steps were conducted using the protocols described above in the purification section.

2.5. NMR spectroscopy

NMR measurements were performed with Avance 500 equipped with a cryogenic triple resonance probe (Bruker, Rheinstetten, Baden-Württemberg, Germany). The 2D ^{1}H–^{15}N HSQC spectra of 0.1–0.3 mM ^{15}N-labeled protein were measured under an array of buffer conditions with variations in pH. All NMR spectra were processed with Bruker Topspin 3.0.

3. Results

3.1. Overexpression and purification of the ESD, the cytoplasmic domain of DraK and full-length DraR

To produce the ESD (28E-124R), the cytoplasmic domain (146R-424R) of DraK, and full-length DraR on a large scale, the proteins were expressed as an N-terminal GST fusion in *E. coli* BL21. Because the ESD of DraK was sensitive to proteolysis during purification, the C-terminal truncated short form ESD (sESD, 28E-115R) of DraK was also constructed without the unstable C-terminal sequence (116S-124R) after determination of the cleavage site (115R-116S) in the ESD by mass spectroscopy (data not shown). After cell lysis by sonication and centrifugation, the proteins were found to be soluble in the supernatant. Most impurities were removed by the GST column, allowing for sufficient purity and stability of the proteins. Following thrombin digestion to remove the GST fusion tag, size-exclusion chromatography resulted in highly pure proteins (Supplementary Fig. S1).

3.2. Autophosphorylation of DraK and phosphotransfer to DraR

To examine the autophosphorylation of DraK and subsequent phosphotransfer to its cognate RR DraR, the cytoplasmic domain of DraK containing the HAMP and kinase domains, but excluding the N-terminal transmembrane domain, and the GST fusion of full-length DraR were overexpressed and purified from *E. coli*. SDS–PAGE analysis indicated a strong radiolabeled signal of autophosphorylation by the cytoplasmic domain of DraK (phospho-DraK, Supplementary data and Fig. S2 lane 1) after a 15 min incubation with [γ-^{32}P]ATP. Upon the addition of DraR into the autophosphorylated DraK reaction mixture, the phosphoryl group was transferred rapidly from DraK to DraR, suggesting that DraK and DraR constitute a cognate sensor kinase and response regulator pair. However, the levels of radiolabeled phospho-DraR decreased with an increase in the reaction time (Supplementary Fig. S2 lanes 2–6). This result indicates that the phosphoryl group of DraR was removed by either its intrinsic instability or the action of DraK. Frequently, a HK plays a role not only in the phosphorylation of its cognate RR but also in the dephosphorylation of the phosphorylated RR, acting as both kinase and phosphatase [20].

3.3. pH-dependent conformational change of the ESD of DraK

Despite the susceptibility of the ESD of DraK to proteolysis, the measurement of its 2D ^{1}H–^{15}N HSQC spectrum was possible at room temperature. Interestingly, the number of peaks and the distribution of the signals are significantly altered with decreasing pH (Fig. 1A–D). The distribution of peaks shows very narrow and low resolution at pH 7.5 (Fig. 1A), whereas the peaks were well dispersed at pH 4.5 (Fig. 1D), suggesting that the secondary structure of the protein may exist predominantly as an α-helical or disordered form (or mixed) at high pH and β-sheet structure may be generated at low pH. The HSQC spectrum at pH 6.5 shows that the number of peaks is almost twice than expected, indicating that two different structures are simultaneously present with a slow exchange rate at this pH. Moreover, the peak intensities for the two different forms are nearly identical at pH 6.0, indicating that the two forms exist in a stoichiometry of nearly 1–1 at pH 6.0 (data not shown). These NMR spectra demonstrate that the conformational change of the ESD of DraK is highly pH sensitive and the protein is more structured in acidic versus alkaline conditions.

To determine whether the C-terminal truncated short form (sESD, 28E-115R) retained the ability to undergo conformational change with varying pH, 2D ^{1}H–^{15}N HSQC spectra were measured at pH 7.5 and pH 4.5. Consistent with the full-length ESD, the short form also demonstrated an identical conformational change with varying pH (Fig. 1E and F). Therefore, the sESD was used for further structural characterization in this report.

3.4. Characterization of secondary structure and transition point of the sESD of DraK at various pH conditions

To characterize the secondary structure of the sESD of DraK and to determine the transition point of the conformational changes, CD spectra were measured at various pH conditions. The CD spectrum at pH 4.3 appeared nearly identical to that of a typical spectrum for a mixed α-helix/β-sheet secondary structure because of a

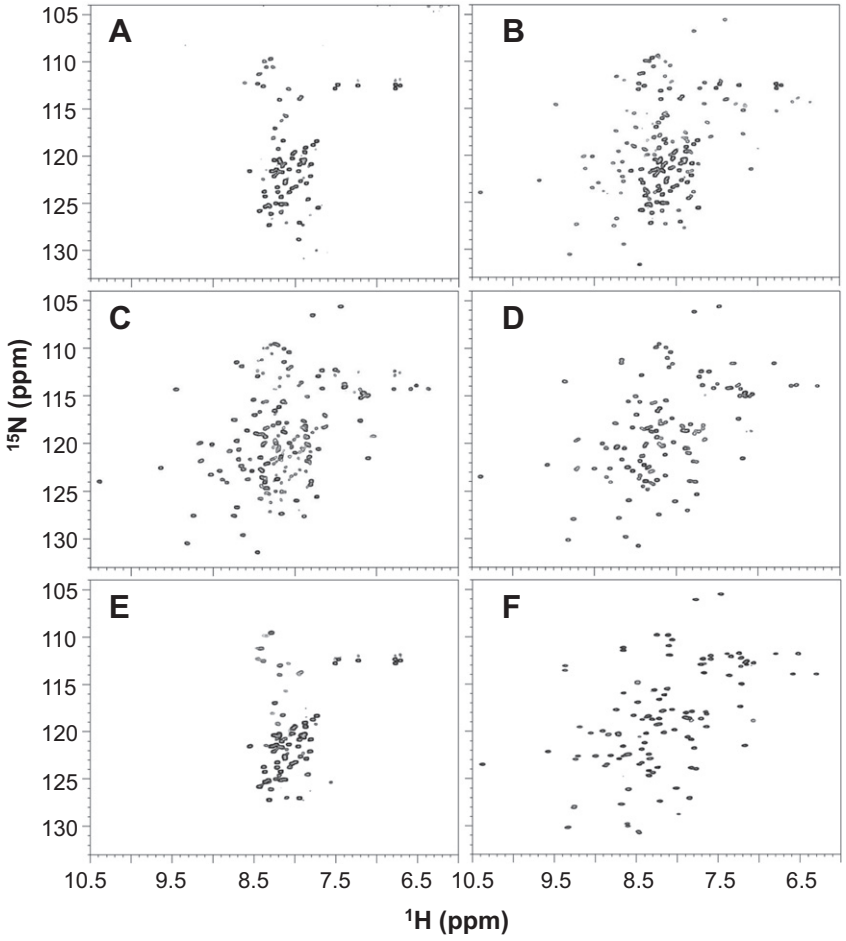

Fig. 1. 2D ^{1}H–^{15}N HSQC NMR spectra of the ESD (A–D) and the sESD (E and F) of DraK at various pH in the presence of 100 mM NaCl. (A) 20 mM HEPES, pH 7.5; (B) 20 mM Bis-tris, pH 6.5; (C) 20 mM Bis-tris, pH 5.5; (D) 20 mM sodium acetate, pH 4.5; (E) 20 mM HEPES, pH 7.5, and (F) 20 mM sodium acetate, pH 4.5.

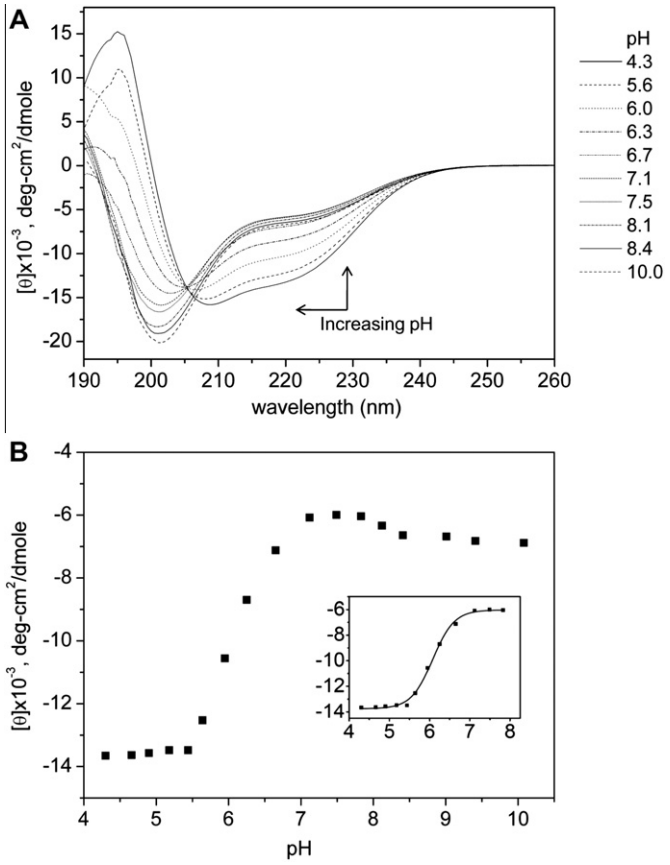

Fig. 2. (A) The CD spectrum of the sESD at each pH condition is represented by different line types. (B) The change in signal intensity at 218 nm over a pH range of 4.3–10.0. The insert shows the sigmoidal curve fitting of a data set of pH 4.3–7.9. The midpoint of the transition occurs at approximately pH 6.1.

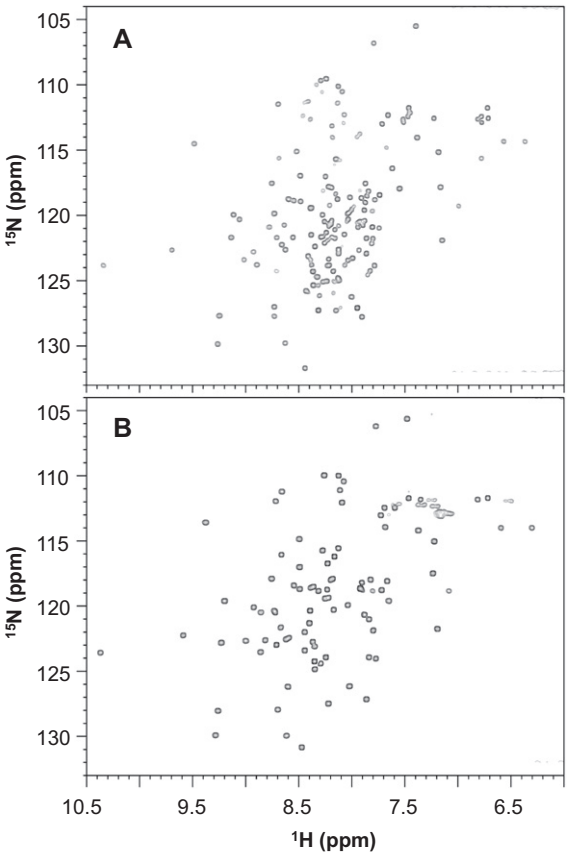

Fig. 3. ^{1}H–^{15}N HSQC spectra of the sESD (E83Q) mutant in 20 mM HEPES, pH 7.5, containing 100 mM NaCl (A) and 20 mM sodium acetate, pH 4.5, containing 100 mM NaCl (B).

single minimum near 208 nm without a minimum near 222 nm, which would be present in an entirely α-helical structure (Fig. 2A). Fig. 2 (A) illustrates that an increase in the pH resulted in a significant change in the secondary structure of the sESD. Between a pH range of 7.0 and 5.0 the intensity near 215 nm, which lies in the region that characteristically displays a minimum for β-sheet, decreased with decreasing pH, suggesting that β-sheet structures are generated by acidic conditions. These results are consistent with those of NMR analysis. At pH 10.0, the minimum peak near 208 nm was shifted to near 200 nm, which is suggestive of a random coil; however, it appears that some α-helical structure remains because the signal near 222 nm is negative and the structural change is reversible below a pH of approximately 10.0. An irreversible change is observed above pH 11. It is conceivable that the structure of the protein is completely destroyed above pH 11. For analysis of the transition points of the conformational changes with varying pH, the signal intensity at 218 nm was monitored. As a result, a distinct transition point appeared at approximately pH 6.1 (Fig. 2B), reflecting that the sESD of DraK distinctly possesses two different conformations between pH 4–10.

3.5. Glutamate residue 83 is a critical residue for the pH-dependent conformational change

Typically, histidine residues influence pH-dependent conformational changes, stability and activity of a protein because the pKa of its side chain is approximately 6.0. Frequently, an abnormally high pKa of glutamate or aspartate side chains induce similar effects in a wide range of pH [21–23]. The ESD of DraK does not contain a histidine residue but possesses 13 glutamates and 6 aspartates. Therefore, the pH-dependent conformational change of the ESD may have occurred by protonation of the side chains of glutamate or aspartate or both residues. We found that the glutamate residue at position 83 is important for the conformational change. The sESD (E83Q) mutant shows well-dispersed ^{1}H–^{15}N correlation peaks above 9.0 ppm at pH 7.5 that are not observed for the wild type at the same pH (Fig. 3). This mutant is expected to behave similarly to the protonated form of the side chain of E83 without the pKa effect of this side chain. This result suggests that the protonation of the E83 side chain is critical for the conformational change of the sESD of DraK. However, the sESD (E83Q) mutant still undergoes pH-dependent conformational change, suggesting that another (or more) acidic residue instead of E83 may be involved in the conformational change. According to the analysis of the CD data, the sESD (E83Q) mutant demonstrates a single transition in the pH range between pH 4.0 and pH 10.0 with the transition point at approximately pH 7.0 shifted approximately 1.0 pH point compared with that of the wild type (Supplementary Fig. S3). Thus, the transition for wild type at approximately pH 6.1 may be caused by the protonation of E83, whereas the transition for the E83Q mutant may be caused by another (or more) acidic residue that has a pKa value higher than that of the side chain of E83 because the transition of the E83Q mutant occurs at approximately pH 7.0. Therefore, protonation of two or more acidic residues in the sESD of DraK could occur during the pH-dependent conformational changes.

3.6. Monomer–dimer equilibrium of the sESD of DraK in solution

It is well known that HKs are functionally homodimers [5,20]. However, many sensor domains of HKs were reported to exist primarily as monomers in solution and in equilibrium between

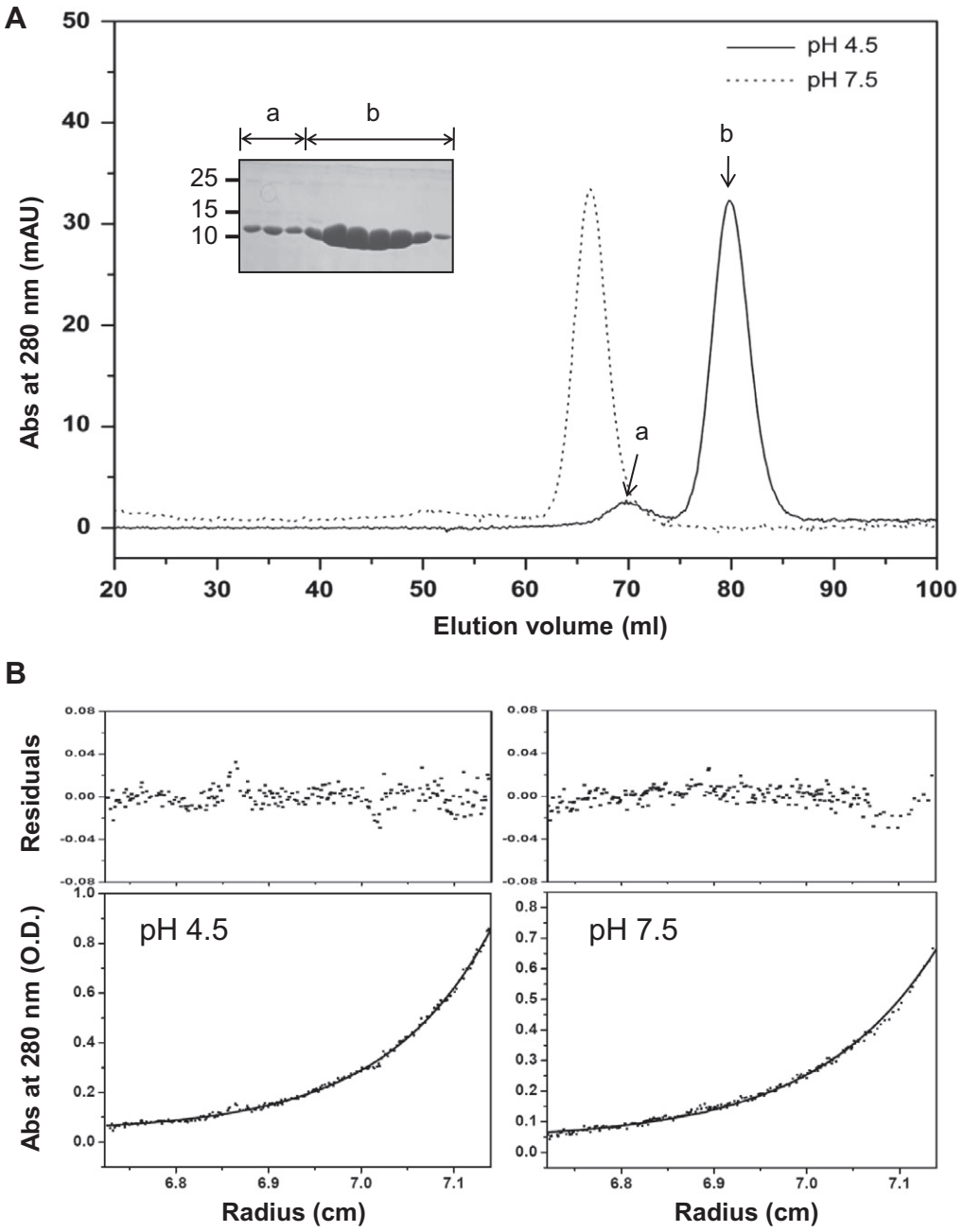

Fig. 4. (A) Size-exclusion chromatography of the sESD (0.2 mM) at pH 4.5 and pH 7.5 containing 100 mM NaCl. Inserts: the SDS–PAGE from the sample at pH 4.5; a represents earlier elution peak and b represents later elution peak. The molecular mass was calculated using standard proteins (see Experimental section). (B) Sedimentation equilibrium data obtained from AUC at pH 4.5 and pH 7.5. The measurement was performed under identical conditions (0.2 mM protein, 30,000 rpm at 4 °C) for both samples. Fitting results (line type) from global analysis of all data sets.

monomer and dimer at high concentration even in the presence of ligand molecules [24,25].

From size-exclusion chromatography, at pH 4.5, the sESD of DraK eluted at 76 mL and 69 mL, which approximates the molecular weight of the sESD monomer (9.7 kDa) and dimer (19.4 kDa), respectively (Fig. 4(A), solid line). However, at pH 7.5, the protein eluted as a single peak at 66 mL, corresponding to a molecular mass of approximately 29 kDa (Fig. 4(A), dashed line). The high molecular weights calculated from size-exclusion chromatography at pH 7.5 are possibly caused by molecular shape due to a more disordered form at pH 7.5.

To estimate the molecular weight of the sESD independently from the molecular shape at each pH, a sedimentation equilibrium experiment using AUC was performed with 0.2 mM protein at pH 4.5 and pH 7.5 (Fig. 4B). Analysis of the AUC data confirms that the protein at pH 4.5 and pH 7.5 sedimented with molecular weights of 10.5 kDa and 9.2 kDa, respectively, close to the expected molecular weight for the monomer of sESD (9.7 kDa). The molecular weight calculated from AUC at pH 4.5 is slightly higher than that of the sESD monomer, meaning that the sESD may exist some dimer at pH 4.5. Together with size-exclusion and experiments, we suggest that the sESD is mainly monomeric in various pH conditions and exists as monomer–dimer equilibrium at acidic condition.

4. Discussion

Bacterial TCSs play central roles in sensing the external stimuli and accordingly regulating the genome-wide expression for

adaptation. Streptomyces is well known as a useful bacterium for the production of natural antibiotics applied in human and veterinary medicine. To date, only a few TCSs in *S. coelicolor* have been functionally characterized and shown to play important roles in secondary metabolism [10–19]. More recently, it has been reported that the DraR/DraK TCS is involved in medium-dependent regulation of the biosynthesis of the antibiotics ACT, yCPK, and RED [19]. However, the signal molecule for the ESD of DraK remains to be identified, and the sensing mechanism is unknown. Therefore, to identify the ligand molecule and to understand the sensing mechanism, structural study of the sensor domain of DraK is highly required. For this purpose, we overexpressed and purified the sESD of DraK and examined its structural characteristics. From 2D $^{1}H–^{15}N$ HSQC NMR spectroscopy, we found that the conformational change of the sESD is highly pH-sensitive, and it appears that β-sheet structure forms at low pH (Fig. 1). Furthermore, $^{1}H–^{15}N$ correlation peaks of two distinctly different conformations are observed simultaneously between pH 5.0–7.0, indicating that two conformations exchange with a slow exchange rate (>10 ms) in solution. In agreement with NMR data, the CD spectra of the sESD suggested that the ESD contains α-helical and disordered structure at high pH and acidic conditions generate β-sheet structure in the structure of the sESD (Fig. 2A). A detailed analysis of the CD spectra indicated that the sESD undergoes transition at a pH of approximately 6.1 (Fig. 2B). From a mutational approach, we found that the glutamate residue at position 83 is critical for the conformational change (Fig. 3). The results suggest that at least two acidic residues (or more) have abnormally high p*K*a values and could be responsible for the pH-dependent conformational change of the sESD. Additionally, our findings from size-exclusion chromatography and AUC analysis indicate that the sESD is predominately monomeric in solution and the dimer of sESD is also present in acidic conditions (Fig. 4).

Although we could not identify the signal molecule of DraK, we believe that our findings could provide information to understand the signal sensing mechanism of DraK HK. To identify the signal molecule of DraK, more detailed functional studies of DraK are required in future studies.

Acknowledgment

We are grateful to Myung Hee Kim for providing the genomic DNA of *Streptomyces coelicolor* A3(2). This work was supported by KBSI grant (T32410) to C.H.K. and Pioneer Research Program for Converging Technology (20110002349), and by The Intelligent Synthetic Biology Center of Global Frontier Project (20110031947) funded by the Ministry of Education, Science and Technology, Republic of Korea.

Appendix A. Supplementary data

Supplementary data associated with this article can be found, in the online version, at http://dx.doi.org/10.1016/j.bbrc.2013.01.018.

References

[1] Y. Gotoh, Y. Eguchi, T. Watanabe, S. Okamoto, A. Doi, R. Utsumi, Two-component signal transduction as potential drug targets in pathogenic bacteria, Curr. Opin. Microbiol. 13 (2010) 232–239.
[2] B.L. Taylor, I.B. Zhulin, PAS Domains: Internal sensors of oxygen, redox potential, and light, Microbiol. Mol. Biol. Rev. 63 (1999) 479–506.
[3] J. Perry, K. Koteva, G. Wright, Receptor domains of two-component signal transduction systems, Mol. BioSyst. 7 (2011) 1388–1398.
[4] J.B. Stock, A.J. Ninfa, A.M. Stock, Protein phosphorylation and regulation of adaptive responses in bacteria, Microbiol. Rev. 53 (1989) 450–490.
[5] J. Cheung, W.A. Hendrickson, Sensor domains of two-component regulatory systems, Curr. Opin. Microbiol. 13 (2010) 116–123.
[6] Z. Zhang, W.A. Hendrickson, Structural characterization of the predominant family of histidine kinase sensor domains, J. Mol. Biol. 400 (2010) 335–353.
[7] S.D. Bentley, K.F. Chater, A.-M. Cerdeño-Tárraga, G.L. Challis, N.R. Thomson, K.D. James, D.E. Harris, M.A. Quail, H. Kieser, D. Harper, et al., Complete genome sequence of the model actinomycete *Streptomyces coelicolor* A3(2), Nature 417 (2002) 141–147.
[8] D.A. Hopwood, Forty years of genetics with Streptomyces: from in vivo through in vitro to in silico, Microbiology 145 (1999) 2183–2202.
[9] M.I. Hutchings, P.A. Hoskisson, G. Chandra, M.J. Buttner, Sensing and responding to diverse extracellular signals? Analysis of the sensor kinases and response regulators of *Streptomyces coelicolor* A3(2), Microbiology 150 (2004) 2795–2806.
[10] A. Yepes, S. Rico, A. Rodríguez-García, R.I. Santamaría, M. Díaz, Novel two-component systems implied in antibiotic production in *Streptomyces coelicolor*, PLoS One 6 (2011) e19980.
[11] D. Rozas, S. Gullón, R.P. Mellado, A novel two-component system involved in the transition to secondary metabolism in *Streptomyces coelicolor*, PLoS One 7 (2012) e31760.
[12] A. Sola-Landa, R.S. Moura, J.F. Martin, The two-component PhoR-PhoP system controls both primary metabolism and secondary metabolite biosynthesis in Streptomyces lividans, Proc. Natl. Acad. Sci. USA 100 (2003) 6133–6138.
[13] A. Sola-Landa, A. Rodríguez-García, E. Franco-Domínguez, J.F. Martín, Binding of PhoP to promoters of phosphate-regulated genes in *Streptomyces coelicolor*: identification of PHO boxes, Mol. Microbiol. 56 (2005) 373–1385.
[14] F. Santos-Beneit, A. Rodríguez-García, A. Sola-Landa, J.F. Martín, Cross-talk between two global regulators in Streptomyces: PhoP and AfsR interactin the control of afsS, pstS and phoRP transcription, Mol. Microbiol. 72 (2009) 53–68.
[15] D. Shu, L. Chen, W. Wang, Z. Yu, C. Ren, W. Zhang, S. Yang, Y. Lu, W. Jiang, AfsQ1-Q2-sigQ is a pleiotropic but conditionally required signal transduction system for both secondary metabolism and morphological development in Streptomyces coelicolor, Appl. Microbiol. Biotechnol. 81 (2009) 1149–1160.
[16] N.L. McKenzie, J.R. Nodwell, Phosphorylated AbsA2 negatively regulates antibiotic production in Streptomyces coelicolor through interactions with pathway-specific regulatory gene promoters, J. Bacteriol. 189 (2007) 5284–5292.
[17] H. Ishizuka, S. Horinouchi, H.M. Kieser, D.A. Hopwood, T. Beppu, A putative two-component regulatory system involved in secondary metabolism in Streptomyces spp, J. Bacteriol. 174 (1992) 7585–7594.
[18] Y. Lu, W. Wang, D. Shu, W. Zhang, L. Chen, Z. Qin, S. Yang, W. Jiang, Characterization of a novel two-component regulatory system involved in the regulation of both actinorhodin and a type I polyketide in Streptomyces coelicolor, Appl. Microbiol. Biotechnol. 77 (2007) 625–635.
[19] Z. Yu, H. Zhu, F. Dang, W. Zhang, Z. Qin, S. Yang, H. Tan, Y. Lu, W. Jiang, Differential regulation of antibiotic biosynthesis by DraR-K, a novel two-component system in *Streptomyces coelicolor*, Mol. Microbiol. 85 (2012) 535–556.
[20] P. Casino, V. Rubio, A. Marina, The mechanism of signal transduction by two-component systems, Curr. Opin. Struct. Biol. 20 (2010) 763–771.
[21] J. Davoodi, W.W. Wakarchuk, R.L. Campbell, P.R. Caarey, W.K. Surewtcz, Abnormally high pK, of an active-site glutamic acid residue in Bacillus circulans xylanase, Eur. J. Biochem. 232 (1995) 839–843.
[22] M. Inoue, H. Yamada, Y. Hashimoto, T. Yasukochi, K. Hamaguchi, T. Miki, T. Horiuchi, T. Imoto, Stabilization of a protein by removal of unfavorable abnormal pKa: Substitution of undissociable residue for glutamic acid-35 in chicken lysozyme, Biochemistry 31 (1992) 8816–8821.
[23] L. Ragona, F. Fogolari, M. Catalano, R. Ugolini, L. Zetta, H. Molinari, EF loop conformational change triggers ligand binding in -lactoglobulins, J. Biol. Chem. 278 (2003) 38840–38846.
[24] C.D. Waldburger, R.T. Sauer, Signal detection by the PhoQ sensor-transmitter, J. Biol. Chem. 271 (1996) 26630–26636.
[25] M.B. Neiditch, M.J. Federle, A.J. Pompeani, R.C. Kelly, D.L. Swem, P.D. Jeffrey, B.L. Bassler, F.M. Hughson, Ligand-Induced asymmetry in histidine sensor kinase complex regulates quorum sensing, Cell 126 (2006) 1095–1108.